Acta Mech 228, 837–849 (2017)
DOI 10.1007/s00707-016-1722-2

ORIGINAL PAPER

Alessandro Baratta · Ileana Corbi · Ottavia Corbi

Theorems for masonry solids with brittle time-decaying tensile limit strength

Received: 3 January 2016 / Revised: 28 June 2016 / Published online: 22 October 2016
© Springer-Verlag Wien 2016

Abstract In this paper, we introduce a phenomenological model approximating the behaviour of masonry structures, which is based on a low-tension elastic–brittle (EB) assumption with evolutionary tensile behaviour. The EB model is conceived by embedding a decaying tensile strength in the material behaviour, and it is able to achieve good agreement with the real behaviour of masonry. Since the model is quite sophisticated, non-holonomic, and the EB solution depends—amongst other things—on the loading path, it is worthwhile to investigate the relationships with more manageable and stable models rather than searching for unreliable solutions that depend on poorly predictable data. Namely, whereas it is quite clear and largely agreed upon that structural models widely applied in engineering (like perfectly plastic or no-tension models or other ones) are well-conditioned problems, the same does not apply to brittle structures. In this case, exact solutions are hard to be found and are scarcely attractive from the engineering point of view since they also depend on the load history and on unverifiable variables such as the local tensile strength. In view of these considerations, in this paper it is proved that stress fields in tensioned EB problems can be approached by highly stable solutions, on the upper and lower sides of the relevant complementary energy, and that the approximation gets closer as the limit tensile strength of the brittle material becomes lower.

Abbreviations

CE	Complementary energy
MCE	Minimum complementary energy
EB	Elastic–brittle
EL	Purely elastic
NT	No-tension
PL	Elastic–plastic
VWP	Virtual work principle

A. Baratta (✉) · I. Corbi · O. Corbi
Department of Structures for Engineering and Architecture, University of Naples Federico II, via Claudio 21, 80125 Naples, Italy
E-mail: alessandro.baratta@unina.it
Tel.: 00390817683739
Fax: 00390817683739

I. Corbi
E-mail: ileana.corbi@unina.it

O. Corbi
E-mail: ottavia.corbi@unina.it

List of symbols

O	Axis origin
s	Curvilinear abscissa
ℓ	Length of the model mid-line
V, S_1	Body volume and constrained part of the body surface
θ	Direction tangent to the barycentre line
$e(s)$	Eccentricity
$h'(s)$, $h''(s)$	Distances of the upper and lower profiles of the arch from the cross-sectional barycentre
$n(s)$	Neutral axis
$A_r(s)$	Resistant part of the cross section
$G_r(s)$	Barycentre of $A_r(s)$
$C(s)$	Solicitation centre
e_r	Distance of C(s) from $G_r(s)$
$d_{Gr}(s)$	Distance of $G_r(s)$ from $n(s)$
ρ	Material density
E	Elastic modulus in compression of the masonry
g, c	Gravity acceleration, fraction of the gravity acceleration
$a_{\max}$	Maximum horizontal ground acceleration
τ, t	Parameter governing the loading process, and one single value
$\mathbf{p}$	Surface loads
$\mathbf{G}$	Body forces
$\mathbf{u}$	Imposed displacement field on S_1
$X_i \ \ (i = 1, 2, 3)$	Unknown static variables (static redundancies)
X_1, X_2, X_3	Thrust force, support force, and bending moment redundancies
$\mathbf{S}_0(s)$, $\mathbf{S}_i(s)$	Stress resultant vectors for the isostatic schemes under the applied loads and the i-th unit redundancy X_i
$N(s)$, $T(s)$, $M(s)$	Normal force, shear force, and bending moment
$N_0(s)$, $T_0(s)$, $M_0(s)$	Stress resultants referred to the isostatic scheme under the applied loads
$N_i(s)$, $T_i(s)$, $M_i(s)$	Stress resultants referred to the isostatic scheme under the i-th unit redundancy X_i
N_d, T_d, M_d	Values of the static redundancies on the basis of the leftward abutment of the portal arch
u_d, v_d, ϕ_d	Settlements of the foundation basis of the leftward abutment of the portal arch
σ	Statically admissible stress
σ_o', ε_o'	Tensile yield stress and strain
σ_θ	Stress component along θ
ε, ε_{e}, ε_{f}	Strain and relevant elastic and fracture components
$\varepsilon_{\mathrm{EB}}$, $\varepsilon_{\mathrm{fEB}}$	EB strain and fracture component
$\mathcal{C}(X_1, X_2, X_3)$	Convex functional over the convex set (X_1, X_2, X_3)
$\mathcal{C}$	Complementary energy functional
D_{EB}, σ_{EB}, $\mathcal{C}_{\mathrm{EB}}$	EB admissible domain, solution stress and complementary energy
D_{EL}, σ_{EL}, $\mathcal{C}_{\mathrm{EL}}$	EL admissible domain, solution stress and complementary energy
D_{NT}, σ_{NT}, $\mathcal{C}_{\mathrm{NT}}$	NT admissible domain, solution stress and complementary energy
D_{PL}, σ_{PL}, $\mathcal{C}_{\mathrm{PL}}$	PL admissible domain, solution stress and complementary energy
$\mathbf{T}$, $\mathbf{T}_{\mathrm{NT}}$	Reactions in equilibrium with any NT statically admissible stress σ and with the stress solution σ_{NT}

1 Introduction

When addressing problems relevant to masonry structures, current assessed mechanical models are often referred to, usually neglecting any skill of the masonry body to resist tensile stresses. The typical NT (no-tension) hypothesis is often coupled to an indefinite resistance to compressive stresses under purely elastic behaviour in compression or otherwise to some ductility in compression. Such models are able to produce reliable theoretical/numerical results whilst offering some further advantages such as an acceptable computa-

tional effort and manageability in civil engineering applications, witnessing the deep research attention on the topic attracted during the last decades by the international scientific community [1–21].

Actually, the problem of performing reliable safety assessment about the behaviour of masonry structures, which mainly depends on the proper choice and implementation of the material mechanical model, is of primary interest. Despite the high number of researches already developed on the subject, it still represents a very central and open research field, still needing great scientific effort. Under this perspective, the material modelling plays a fundamental role. The analysis and theoretical treatment of masonry constructions often pushes towards the adoption of more sophisticated mechanical models for masonry continua, aiming at embedding, for instance, orthotropic behaviour, crushing in compression, cohesive, and/or frictional behaviour in shear, with strength depending on the level of vertical compression, influence of the effective masonry arrangement, and so on. In general, such models may be more accurate in principle but are less treatable and they are also much less reliable in practice, depending on many uncertain parameters and properties. One should also distinguish some features that may be easily overcome, like the limit in compression, from some other features, like the orthotropic behaviour, that may be very interesting for analysis purposes giving place to further theoretical ad hoc treatments, but are quite inessential on the side of field engineering.

One feature requiring a specific analytical treatment is represented by the brittleness in tension of the stone/mortar assemblage, which is the object of the paper and that represents, or may represent, a significant weakness in the structural assessment of masonry structures. All choices relevant to the proper planning and application of the most appropriate interventions for the effective protection of the monumental heritage, also by means, for example, of dynamic control strategies and new refurbishment techniques [22–26], need to be based on reliable models.

The no-tension assumption for masonry solids is mainly supported by the circumstance that, even if some (most times low) resistance to tensile stresses may exist in masonry, it is neither reliable nor exactly predictable since it is point-dependent and it usually decays with time and after stress peaks (brittle behaviour). A more realistic mechanical model may therefore be built up, able to take into account such, possibly low, skill of the material body to resist tensile stresses, embedding the brittleness in tension and thus improving the performance of the NT models when applied to the analysis of masonry structures. Obviously, such a variant of the reference NT model is expected to involve some increased computational effort and makes more complex the implementation and the handling of the model for usual investigations.

To this regard, in the following an elastic–brittle tension-resistant model (EB) exhibiting an evolutionary behaviour with a decay of the tensile resistance after stress peaks is illustrated. Because of its major complexity with respect to the standard NT models, due to the tensile behaviour practically evolving towards the no-tension behavior and the above-reported considerations about the increased numerical effort, investigations are required about procedures for searching the solutions and about assessment of stability. On the other hand, the EB model solution should be properly explored in order to evaluate the overall improvements possibly deriving from the assumption of this more sophisticated behaviour of masonry with respect to the NT solution. This is also required by the circumstance that, on one hand, a complete settlement of the NT theory is not yet achieved, and, as mentioned, further studies are still needed for solving a number of problems, for example, relevant to the still lacking availability of commercial NT software, or to the analysis of complex double curvature NT surfaces as in the case of masonry vaults, but on the other hand these problems become more and more complex when based on further sophisticated material models like, precisely, when brittle fracture phenomena are taken into account.

In the set-up of the presented EB model, some non-null tensile resistance is considered, thus admitting the occurrence of some tensile stresses in the material body, and an elastic–brittle behaviour in tension is coupled to indefinite elastic behaviour in compression. The model may be also enriched in a subsequent research stage, admitting some ductility in compression, as in the case of NT material. Differently from the NT material, the EB model is characterised by an evolutionary resistance domain which, after occurrence of fractures, decays towards the NT domain. Even in the EB model, like in the NT one, the fracture is assumed to be co-axial with the stress state and some elastic re-entries are possible after the closure of fractures, by re-acquiring some skill of reacting to tangent stresses. Thereafter, some exploration of the properties of the EB solution is presented in the paper under the energetic profile, and comparisons with solutions relevant to other material models, such as the NT solution, are developed in order to evaluate the opportunity and feasibility of adopting the EB model.

The results of the developed theoretical investigation which is carried on in the paper allow to achieve some final considerations about the convenience in adopting more complex phenomenological models, but also allowing to evaluate to what extent the real behaviour of the structure depends on its loading history.

2 The NT model for masonry under mono-axial stress states

2.1 The problem set-up for NT portal arches and vaults

In structural patterns like masonry portal arches and vaults, as shown for example for the case of a single span portal arch in Fig. 1, the equilibrium between the internal stresses and the applied loads coupled to the admissibility condition of the NT material, which is unable to resist tensile stresses, would require that the internal resultants' funicular line is included in the thickness of the portal arch (or vault).

The shear stress on any cross section of the arch and of the piers is, then, small in comparison with the normal internal force, since the pressure line should be contained inside the profile of the structure; otherwise, the structure would be at or over the collapse threshold, and no solution can exist. Therefore, it is common practice to neglect the influence of the shear stress on the stress admissibility at any cross section, and one can assume that the stress state is mono-axial at any point (i.e. the resultant force on any cross section is approximately orthogonal to the section itself). This assumption results in a significant simplification of the cross-sectional stress state, which may be assumed as mono-axial. Therefore, when adopting the NT (no-tension) assumption, one may search for the NT solution by a stress approach based on the constrained minimisation of a suitably defined complementary energy functional [8]. In such cases, the set of stress fields equilibrating the applied loads can be built up by superposition whilst the stress field can be associated with the internal forces on every cross section by a bi-linear distribution pattern as shown on the right side of Fig. 1. The overall structural system is characterised by only three static redundancies, so that the number of static unknowns is much smaller than the number of kinematic ones and a force approach turns the most convenient and practicable. The solution of the structural problem, in this case, can be best approached through the minimum principle of complementary energy, and the procedure is aimed at identifying the redundant reactions allowing constraint compatibility whilst minimising the complementary energy functional, whose expression is inferred by the introduced stress distribution.

In detail, let us refer to the single span portal arch model subject to a load pattern shown in Fig. 1, in the xy-plane. In the following, vectors and tensors are denoted in bold. Let consider the loads represented by surface forces $\mathbf{p}$ acting on the arcade and body forces $\mathbf{G}$, both due to gravity acceleration g and to a possible field of horizontal base accelerations

$$\mathbf{p} = \begin{bmatrix} p_x \\ p_y \end{bmatrix} = \begin{bmatrix} cp \\ p \end{bmatrix} = p \begin{bmatrix} c \\ 1 \end{bmatrix}, \quad \mathbf{G} = \begin{bmatrix} G_x \\ G_y \end{bmatrix} = \begin{bmatrix} -a_{\max} \\ -g \end{bmatrix} = -\rho g \begin{bmatrix} c \\ 1 \end{bmatrix}, \tag{1}$$

with ρ denoting the (constant) material density, and $a_{\max}$ the maximum horizontal ground acceleration, set equal to a fraction c of the gravity acceleration.

Equilibrium stress fields can be built up from stress resultant fields. At the generic curvilinear abscissa s on the model mid-line (with origin in O), the stress resultants on the relevant cross section in terms of shear force, normal force, and bending moment are denoted by $T(s)$, $N(s)$, and $M(s)$, respectively.

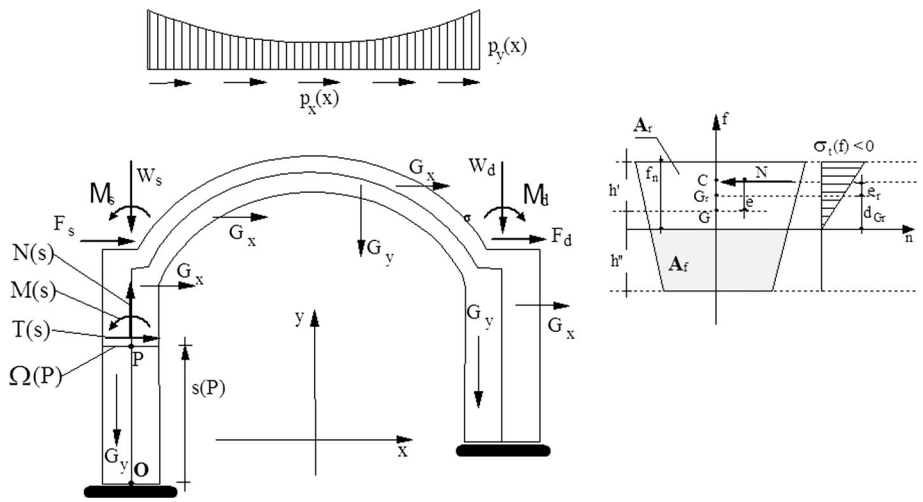

Fig. 1 Portal arch model with the bi-linear stress pattern at the generic cross section

Since the structure is characterised by three static redundancies, the set of stress fields equilibrating the applied loads can be built up by a superposition scheme, where three redundant stress components are recognised in the thrust force X_1, the support force X_2, and the bending moment X_3 at the section where the arch is supported by the abutment on the left. Once collected the stress resultants at the generic abscissa in a vector $\mathbf{S}(s) = [T(s)\ \ N(s)\ \ M(s)]^T$, one can build up by superposition the stress field in equilibrium with the applied loads for any value of the unknown static variables X_i for $i = 1, 2, 3$ as follows:

$$\mathbf{S}(s) = \mathbf{S}(s|X_1, X_2, X_3) = \mathbf{S}_0(s) + \sum_{i=1}^{3} X_i \mathbf{S}_i(s), \tag{2}$$

where $\mathbf{S}_0(s)$ represents the stress resultant vector at the considered curvilinear abscissa corresponding to the applied loads, whilst $\mathbf{S}_i(s)$ denotes the one relevant to i-th pattern where the i-th static unknown X_i is assumed equal to unit.

On the other side, the condition for static admissibility requires that the same fields do not violate the condition for the resistance of the material. One should consider that, for static admissibility, the thrust line must be internal to the profile of the arch, so that for any cross section the stress resultant forms a small angle with respect to the mid-line, and the shear force results to be small with respect to the normal force. If one neglects the influence of the shear stress on the stress admissibility at any point, one can assume that the stress state σ is mono-axial at any point Q in the volume V (i.e. the resultant force on any cross section is orthogonal to the section itself) and the resistance condition may be written in the form

$$\sigma_\theta(Q) \leq 0 \quad \forall Q \in V, \tag{3}$$

where θ denotes the direction tangent to the barycentre line at the point where the cross section containing Q intersects the barycentre line.

The admissibility of the stress field is then guaranteed by the condition that the force resultant line is everywhere in the interior of the arch profile; this condition implies that the eccentricity $e(s)$ (which is given by $e(s) = M(s)/N(s)$) of the stress resultant $N(s)$, at the generic curvilinear abscissa, is required to be bounded by the distances $h'(s)$ and $h''(s)$ of the upper and lower profiles of the arch from the cross-sectional barycentre (Fig. 1).

The NT admissibility conditions may be written in the form

$$\begin{cases} N(s) \leq 0 \\ -h'(s) \leq \frac{M(s)}{N(s)} \leq h''(s) \end{cases} \quad \forall s \in (0, \ell), \tag{4}$$

where ℓ is the length of the model mid-line.

2.2 The MCE approach for NT arches, portal arches, and vaults

By the minimum complementary energy (MCE) approach, the NT solution of the stress problem should be searched for in the class of the equilibrated and NT admissible solutions. Within the set of statically admissible solutions, the MCE functional attains its minimum in solution [11]. Consequently, the NT stress solution can be achieved by solving a suitably set up constrained minimum problem that, for NT structures under mono-axial stress state, is expressed in the following form:

$$\begin{cases} \text{Find} \min_{X_1, X_2, X_3} \mathcal{C}(X_1, X_2, X_3) = \frac{1}{2} \int_0^\ell \frac{N^2(s)}{EA_r(s)} \left(1 + \frac{e_r(s)}{d_{Gr}(s)}\right) \mathrm{d}s - N_d u_d - T_d v_d - M_d \phi_d \\ \text{Sub} \begin{cases} \text{equilibrium} \begin{cases} N(s) = N_0(s) + \sum_{i=1}^3 X_i N_i(s) \\ T(s) = T_0(s) + \sum_{i=1}^3 X_i T_i(s) \\ M(s) = M_0(s) + \sum_{i=1}^3 X_i M_i(s) \end{cases} \quad \forall s \in (0, \ell) \\ \text{admissibility} \begin{cases} N(s) \leq 0 \\ -h'(s) \leq \frac{M(s)}{N(s)} \leq h''(s) \end{cases} \end{cases} \end{cases} \tag{5}$$

where E denotes the elastic modulus in compression of the masonry, e_r is the distance of the solicitation centre $C(s)$ from the barycentre $G_r(s)$ of the resistant part $A_r(s)$ of the cross section, and $d_{Gr}(s)$ denotes the distance

of $G_r(s)$ from the neutral axis $n(s)$ (as shown in Fig. 1). Moreover, $N_d = N(0)$, $T_d = T(0)$, $M_d = M(0)$ denote, respectively, the values assumed by the static redundancies on the basis of the leftward abutment, and u_d, v_d, ϕ_d the settlements of the foundation basis of the leftward abutment; $N_0(s)$, $T_0(s)$, $M_0(s)$ represent the stress resultants referred to the isostatic scheme under the applied loads, whereas $N_i(s)$, $T_i(s)$, $M_i(s)$ represent the stress resultants referred to the isostatic scheme under the i-th static redundancy X_i assumed equal to the unit.

The constraint conditions set in Eq. (5) can be observed to be of linear type. The minimum of the convex functional $\mathcal{C}(X_1, X_2, X_3)$ over the convex set $\mathbf{X}$ defined by the linear inequalities given in Eq. (5) represents a problem of convex optimisation. Because of the convexity of $\mathcal{C}(X_1, X_2, X_3)$, if the admissible set $\mathbf{D}_{\mathrm{NT}}$ is not empty, the NT solution exists and is unique. If, on the contrary, no solution exists for the inequalities in Eq. (5), the set $\mathbf{D}_{\mathrm{NT}}$ is empty, since no purely compressive stress distribution on the cross section can equilibrate a force applied at a point exterior to the section. Therefore, in this case, although the inequalities in Eq. (5) are written with reference to a particular stress pattern, no other stress pattern can hold.

By the principles of masonry limit analysis if no solution exists for Eq. (5), the structure is over the failure condition in the sense of the static theorem. However, it is worthwhile to notice that the limit analysis in the sense of the kinematical theorem can be viewed at more as a test for the existence of solutions rather than as a tool for the safety assessment. Collapse mechanisms associated with unilateral hinges activation, in fact, can hardly be associated with admissible values of stress, and/or if plasticity is assumed in compression, ductility of masonry is a hope rather than a fact.

3 Relationships of the stress solutions under different material assumptions

3.1 Selection of mechanical models: purely elastic, elastic–plastic, no-tension, and elastic–brittle low tension

As shown in the previous section, in structures of the type of arches, portal arches, and vaults under investigation, one may neglect the influence of the shear stress on the stress admissibility at any point, and one assumes that the stress state is mono-axial at any point. The stress solution is thus desirable since it represents the fastest way to pursue the solution with the lowest computational effort, by performing a complementary energy minimisation under the admissibility conditions relevant to the adopted material model.

In the following, we consider four different mechanical models of the material, i.e. (i) the no-tension (NT) model, (ii) the purely elastic (EL) model, (iii) the elastic–brittle (EB) low-tension model, and (iv) the elastic–plastic (PL) model, in order to analyse the relationships existing between the relevant stress solutions. The stress–strain diagrams for the four models are reported in Fig. 2. One should emphasise that some of the mentioned mechanical models are unreliable when applied to the masonry material (like in the case of the elastic assumption and, even more, in the case of the elastic–plastic one) and, therefore, their investigation should be considered of purely academic interest if not critically correlated to the behaviour of the problem at hand. Anyway, one should emphasise that available commercial software based on such assumptions is often forced to comply with the masonry behaviour, and, thus, some practical interest arises in deepening the matter.

3.2 The no-tension solution as a constrained minimum of the complementary energy functional

Under the NT hypothesis, the material obeys a number of conditions regarding the stress σ and the strain ε, composed by an elastic and fracture component, ε_{e} and ε_{f}, which express the conditions that allow or do not allow the development of the fractures. For NT admissibility, the fracture strain is required to be non-negative, which means that only detachment is allowed. Besides, the stress is required to be non-positive, that is to say purely compressive.

Thus, first of all, one has

$$\varepsilon = \varepsilon_{\mathrm{e}} + \varepsilon_{\mathrm{f}}, \quad \varepsilon_{\mathrm{e}} = \frac{\sigma}{E}, \quad \left.\begin{array}{l} \varepsilon_{\mathrm{f}} \geq 0 \\ \sigma \leq 0 \end{array}\right\} \Rightarrow \sigma \cdot \varepsilon_{\mathrm{f}} \leq 0. \tag{6}$$

The development of fractures and the local detachment along a plane surface at a point can only occur when no stress acts on that surface. Therefore, marking by σ_{NT} the solution stress, the following conditions apply in the solution:

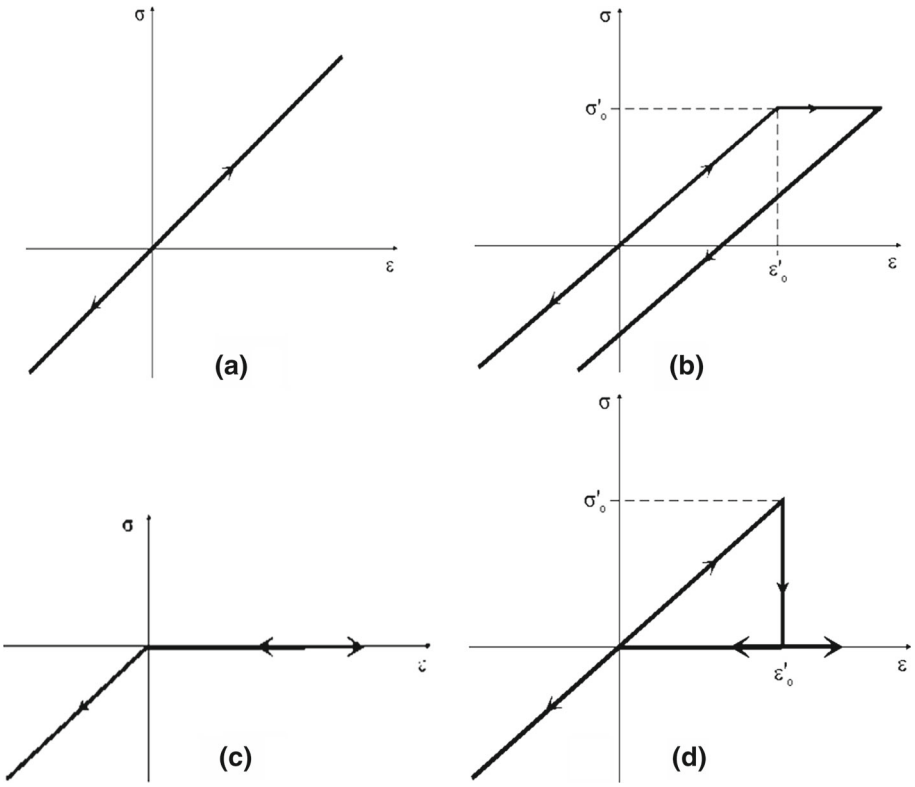

Fig. 2 Mechanical models for the masonry material body. **a** Elastic. **b** Elastic–plastic. **c** No-tension. **d** Elastic–brittle low tension

$$\left.\begin{array}{l}\sigma_{\mathrm{NT}}=0\Rightarrow\varepsilon_{\mathrm{e}}=0,\varepsilon_{\mathrm{e}}=\frac{\sigma_{\mathrm{NT}}}{E}\\ \varepsilon_{\mathrm{f}}>0\Rightarrow\sigma_{\mathrm{NT}}=0\\ \sigma_{\mathrm{NT}}<0\Rightarrow\varepsilon_{\mathrm{f}}=0\end{array}\right\}\Rightarrow\sigma_{\mathrm{NT}}\cdot\varepsilon_{\mathrm{f}}=0 \tag{7}$$

After introducing the reactions $\mathbf{T}_{\mathrm{NT}}$ and $\mathbf{T}$ equilibrated, respectively, by the stress solution σ_{NT} and by any NT statically admissible stress σ, one may introduce the expressions of the CE (complementary energy) functional for the two cases, denoted by $\mathcal{C}_{\mathrm{NT}}$ and $\mathcal{C}$ (dependence on the stress field is omitted), and they are as follows:

$$\mathcal{C}_{\mathrm{NT}}=\frac{1}{2E}\int_V\sigma_{\mathrm{NT}}^2\mathrm{d}V-\int_{S_1}\mathbf{T}_{\mathrm{NT}}\cdot\mathbf{u}\mathrm{d}S,\quad\mathcal{C}=\frac{1}{2E}\int_V\sigma^2\mathrm{d}V-\int_{S_1}\mathbf{T}\cdot\mathbf{u}\mathrm{d}S, \tag{8}$$

where $\mathbf{u}$ is the field of the constrained displacements on the constrained part S_1 of the surface of the body with volume V. One may show that the difference $\Delta\mathcal{C}=\mathcal{C}-\mathcal{C}_{\mathrm{NT}}$ is non-negative for any statically admissible stress field and the CE functional attains its minimum in solution. To this aim, one starts from the application of the VWP (virtual work principle). One considers any admissible stress field given by the difference $(\sigma-\sigma_{\mathrm{NT}})$ in equilibrium with the reactive force field $(\mathbf{T}-\mathbf{T}_{\mathrm{NT}})$, and, on the other side, the solution strain ε compatible with the field of the constrained displacements $\mathbf{u}$ that satisfy the kinematic constraints on the surface S_1. One thus gets

$$\begin{aligned}&\int_V(\sigma-\sigma_{\mathrm{NT}})\cdot\varepsilon\mathrm{d}V=\int_{S_1}(\mathbf{T}-\mathbf{T}_{\mathrm{NT}})\cdot\mathbf{u}\mathrm{d}S\\ &\rightarrow\int_V(\sigma-\sigma_{\mathrm{NT}})\cdot\varepsilon_e\mathrm{d}V+\int_V(\sigma-\sigma_{\mathrm{NT}})\cdot\varepsilon_f\mathrm{d}V=\int_{S_1}(\mathbf{T}-\mathbf{T}_{\mathrm{NT}})\cdot\mathbf{u}\mathrm{d}S\\ &\rightarrow\frac{1}{E}\int_V(\sigma-\sigma_{\mathrm{NT}})\cdot\sigma_{\mathrm{NT}}\mathrm{d}V+\int_V\sigma\cdot\varepsilon_f\mathrm{d}V=\int_{S_1}(\mathbf{T}-\mathbf{T}_{\mathrm{NT}})\cdot\mathbf{u}\mathrm{d}S.\end{aligned} \tag{9}$$

Thereafter, one substitutes Eq. (9) in the expression of the relevant variation in the complementary energy functional, and since from Eq. (6) one has that $\sigma \cdot \varepsilon_f \leq 0$, one finally gets

$$\Delta\mathcal{C} = \mathcal{C} - \mathcal{C}_{\mathrm{NT}} = \frac{1}{2E}\int_V \left(\sigma^2 - \sigma_{\mathrm{NT}}^2\right) \mathrm{d}V - \int_{S_1} (\mathbf{T} - \mathbf{T}_{\mathrm{NT}}) \cdot \mathbf{u}\mathrm{d}S$$
$$= \frac{1}{2E}\int_V (\sigma_{\mathrm{NT}} - \sigma)^2 \,\mathrm{d}V - \int_V \sigma \cdot \varepsilon_f \mathrm{d}V \geq 0. \tag{10}$$

Equation (10) demonstrates that the mentioned energetic functional's variation is non-negative $\Delta\mathcal{C} \geq 0$ for any admissible variation in the stress field imposed starting from the solution, and, therefore, that $\mathcal{C} \geq \mathcal{C}_{\mathrm{NT}}$. Therefore, since $\mathcal{C} \geq \mathcal{C}_{\mathrm{NT}}$, the NT complementary energy functional in solution attains a value that is always upper-bounded by the one relevant to any other NT statically admissible stress field, i.e. by any stress field that equilibrates the applied loads and satisfies the NT material admissibility conditions identifying the NT solution domain $\mathbf{D}_{\mathrm{NT}}$.

The NT stress solution is then characterised by the constraint minimum of the CE functional

$$\sigma_{\mathrm{NT}} : \mathcal{C}_{\mathrm{NT}} = \mathcal{C}(\sigma_{\mathrm{NT}}) = \min_{\sigma \in \mathbf{D}_{\mathrm{EL}} \cap \mathbf{D}_{\mathrm{NT}}} \mathcal{C}(\sigma), \tag{11}$$

where $\mathbf{D}_{\mathrm{EL}}$ represents the purely elastic solution domain where no constraints do apply.

This circumstance allows the specialisation of the problem for the search of the solution for the cases at hand, like in Sect. 3.1 with regard to arches.

3.3 Comparison of the purely elastic solution with the no-tension solution in energetic terms

Since the stress solution σ_{EL} in case of linear elastic behaviour of the continuum would be characterised, in turn, by the minimum $\mathcal{C}_{\mathrm{EL}}$ of the complementary energy under the only constraint imposed by the equilibrium with the applied loads

$$\sigma_{\mathrm{EL}} : \mathcal{C}_{\mathrm{EL}} = \mathcal{C}(\sigma_{\mathrm{EL}}) = \min_{\sigma \in \mathbf{D}_{\mathrm{EL}}} \mathcal{C}(\sigma), \tag{12}$$

one may infer that the NT solution is lower-bounded by the linear elastic one in its definition domain

$$\mathcal{C}_{\mathrm{EL}} \leq \mathcal{C}_{\mathrm{NT}}. \tag{13}$$

In Fig. 3a, the contour lines of the objective function represented by the complementary energy functional are depicted together with the purely elastic stress solution, which coincides with the absolute minimum of the functional. In Fig. 3c, the NT admissibility domain is represented as well, with the identification of the relevant NT solution placed on the boundary of such domain at the point minimising the energy functional.

3.4 Properties of the elastic–brittle low-tension solution and its comparison with the no-tension solution in energetic terms

Although it is temporary because of time decay and brittleness, some tensile resistance, possibly low, may be usually exhibited by the masonry, and it might be embedded in a more realistic mechanical model. The formulation of an EB low-tension (elastic–brittle) behaviour should represent an improvement of the NT modelling, and it is of some interest to investigate the relationships between the two solutions. One thus adopts a brittle behaviour in tension of the type depicted in Fig. 2d.

After denoting by τ the parameter governing the loading process (e.g. the time variable), and, for any value t of τ, one gets

$$\sigma(t) = \begin{cases} E\varepsilon(t) & \text{if} \quad \begin{cases} \varepsilon(t) \leq 0 \\ \text{or} \\ \max\limits_{0 \leq \tau \leq t} \varepsilon(\tau) \leq \varepsilon_o' \end{cases} \\ 0 & \text{if} \quad \begin{cases} \varepsilon(t) \geq 0 \\ \text{and} \\ \max\limits_{0 \leq \tau \leq t} \varepsilon(\tau) > \varepsilon_o' \end{cases} \end{cases} \tag{14}$$

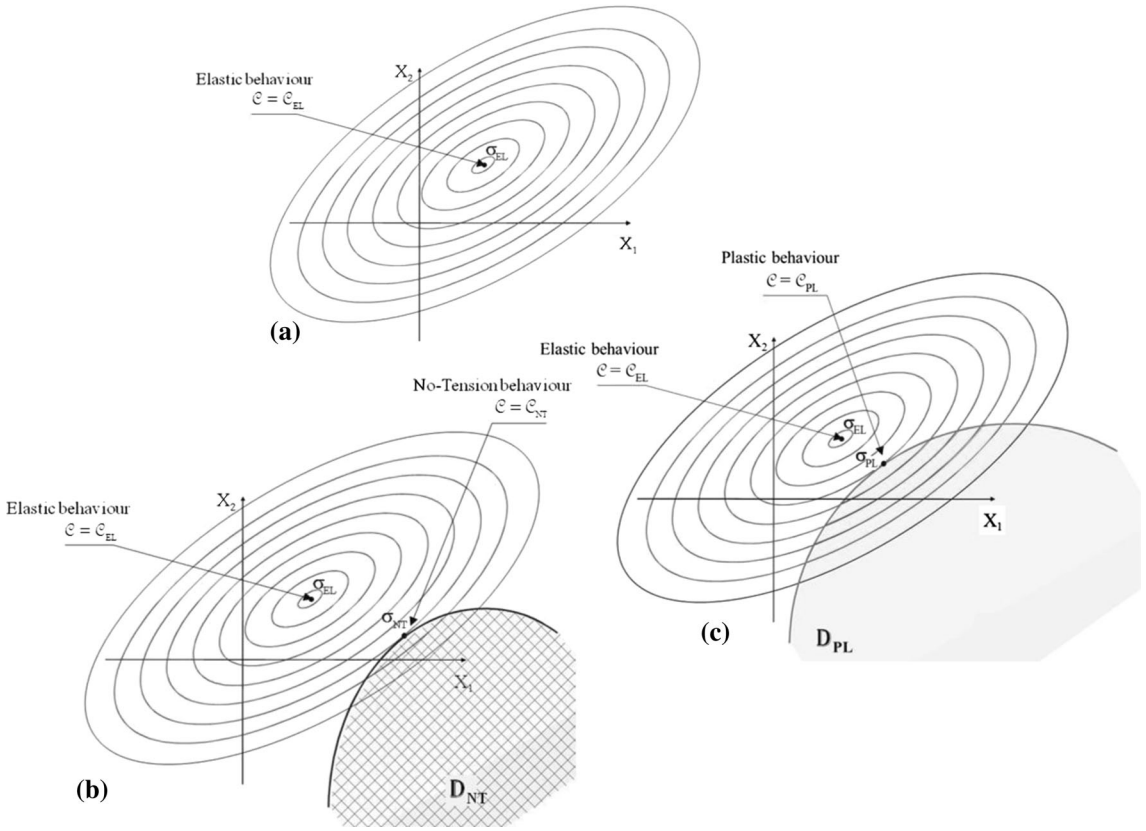

Fig. 3 Energetic properties of: **a** the purely elastic (EL) solution; **b** the no-tension (NT) solution; **c** the elastic-plastic (PL) solution

with ε'_o the yield positive strain.

One should notice that, also in this case, one has that the work of fracture is null:

$$\sigma\,(t)\cdot\varepsilon_f\,(t)=0\quad\forall t. \tag{15}$$

Denoting by σ_{NT} and $\mathcal{C}_{\mathrm{NT}}$, respectively, the stress and the complementary energy attained in the NT solution, and by σ_{EB} and $\mathcal{C}_{\mathrm{EB}}$ the same quantities relevant to the low-tension elastic–brittle solution, after developing some algebraic operations, one can show that

$$\mathcal{C}_{\mathrm{NT}}\geq\mathcal{C}_{\mathrm{EB}}. \tag{16}$$

Actually, denoting all variables relevant to the EB (low-tension elastic brittle) solution by the index $(\cdot)_{\mathrm{EB}}$, one may calculate the difference between to the NT and EB solutions in energetic terms as follows:

$$\mathcal{C}_{\mathrm{NT}}=\frac{1}{2E}\int\limits_V\sigma^2_{\mathrm{NT}}\mathrm{d}V-\int\limits_{S_1}\mathbf{T}_{\mathrm{NT}}\cdot\mathbf{u}\mathrm{d}S,\quad\mathcal{C}_{\mathrm{EB}}=\frac{1}{2E}\int\limits_V\sigma^2_{EB}\mathrm{d}V-\int\limits_{S_1}\mathbf{T}_{\mathrm{EB}}\cdot\mathbf{u}\mathrm{d}S, \tag{17}$$

$$\Delta\mathcal{C}=\mathcal{C}_{\mathrm{NT}}-\mathcal{C}_{\mathrm{EB}}=\frac{1}{2E}\int\limits_V\left(\sigma^2_{\mathrm{NT}}-\sigma^2_{\mathrm{EB}}\right)\mathrm{d}V-\int\limits_{S_1}\left(\mathbf{T}_{\mathrm{NT}}-\mathbf{T}_{\mathrm{EB}}\right)\cdot\mathbf{u}\mathrm{d}S. \tag{18}$$

By applying the VWP to stresses $(\sigma_{\mathrm{NT}}-\sigma_{\mathrm{EB}})$ and forces $(\mathbf{T}_{\mathrm{NT}}-\mathbf{T}_{\mathrm{EB}})$ equilibrating null external loads and to the strains $\varepsilon_{\mathrm{EB}}$ and displacements $\mathbf{u}$, one gets

$$\int\limits_V\left(\sigma_{\mathrm{NT}}-\sigma_{\mathrm{EB}}\right)\cdot\varepsilon_{\mathrm{EB}}\mathrm{d}V=\int\limits_{S_1}\left(\mathbf{T}_{\mathrm{NT}}-\mathbf{T}_{\mathrm{EB}}\right)\cdot\mathbf{u}\mathrm{d}S. \tag{19}$$

Whence, after substitution, one gets

$$\Delta\mathcal{C} = \mathcal{C}_{\mathrm{NT}} - \mathcal{C}_{\mathrm{EB}} = \frac{1}{2E}\int_V \left(\sigma_{\mathrm{NT}}^2 - \sigma_{\mathrm{EB}}^2\right) \mathrm{d}V - \int_V (\sigma_{\mathrm{NT}} - \sigma_{\mathrm{EB}}) \cdot \varepsilon_{\mathrm{EB}} \mathrm{d}V. \tag{20}$$

Since

$$\varepsilon_{\mathrm{EB}} = \frac{\sigma_{\mathrm{EB}}}{E} + \varepsilon_{\mathrm{fEB}}, \tag{21}$$

with $\varepsilon_{f\mathrm{EB}}$ the fracture strain in the EB case, from Eq. (20) one gets

$$\Delta\mathcal{C} = \mathcal{C}_{\mathrm{NT}} - \mathcal{C}_{\mathrm{EB}} = \frac{1}{2E}\int_V \left(\sigma_{\mathrm{NT}}^2 - \sigma_{\mathrm{EB}}^2 - 2\sigma_{\mathrm{NT}}\sigma_{\mathrm{EB}} + 2\sigma_{\mathrm{EB}}^2\right) \mathrm{d}V - \int_V (\sigma_{\mathrm{NT}} - \sigma_{\mathrm{EB}}) \cdot \varepsilon_{\mathrm{fEB}} \mathrm{d}V, \tag{22}$$

and finally

$$\Delta\mathcal{C} = \mathcal{C}_{\mathrm{NT}} - \mathcal{C}_{\mathrm{EB}} = \frac{1}{2E}\int_V \left(\sigma_{\mathrm{NT}} - \sigma_{\mathrm{EB}}\right)^2 \mathrm{d}V - \int_V \left(\sigma_{\mathrm{NT}}\varepsilon_{\mathrm{fEB}} - \sigma_{\mathrm{EB}}\varepsilon_{\mathrm{fEB}}\right) \mathrm{d}V. \tag{23}$$

One observes that the quadratic term in Eq. (23) cannot be negative, whilst the product $\sigma_{\mathrm{NT}} \cdot \varepsilon_{\mathrm{fEB}}$ cannot be positive; moreover, the product $\sigma_{\mathrm{EB}} \cdot \varepsilon_{\mathrm{fEB}}$ is always zero. This implies that the considered variation in the functional is non-negative:

$$\Delta\mathcal{C} = \mathcal{C}_{\mathrm{NT}} - \mathcal{C}_{\mathrm{EB}} = \frac{1}{2E}\int_V \left(\sigma_{\mathrm{NT}} - \sigma_{\mathrm{EB}}\right)^2 \mathrm{d}V - \int_V \sigma_{\mathrm{NT}}\varepsilon_{\mathrm{fEB}} \mathrm{d}V \geq 0. \tag{24}$$

Therefore, in case of non-null tensile resistance ($\sigma_o' > 0$), i.e. of elastic–brittle low-tension material, the relevant complementary energy in the solution is lower than the one relevant to the no-tension resistance case, and they are as follows:

$$\begin{aligned} \Delta\mathcal{C} = \mathcal{C}_{\mathrm{NT}} - \mathcal{C}_{\mathrm{EB}} \geq 0 \\ \Rightarrow \mathcal{C}_{\mathrm{NT}} \geq \mathcal{C}_{\mathrm{EB}}. \end{aligned} \tag{25}$$

Since the energetic solution $\mathcal{C}_{\mathrm{EL}}$ relevant to the indefinitely linear elastic behaviour without any bound on the tensile resistance minimises the energetic functional within the set of stress fields equilibrating the applied loads, one may infer the following order between the three complementary energies in the solution:

$$\mathcal{C}_{\mathrm{NT}} \geq \mathcal{C}_{\mathrm{EB}} \geq \mathcal{C}_{\mathrm{EL}} \tag{26}$$

As a consequence, the elastic–brittle solution is demonstrated to be closer, in terms of complementary energy, to the purely elastic one than the NT solution, and it may therefore be considered more realistic. In Fig. 3a, the contour lines of the objective CE function are depicted together with the purely elastic stress solution, which coincides with the absolute minimum of the functional. The NT admissibility domain is represented as well in Fig. 3b, with the identification of the relevant NT solution placed on the boundary of such domain at the point minimising the energy functional.

3.5 Comparison of the holonomic elastic–plastic solution with the elastic–brittle solution in energetic terms

As mentioned in the above, the elastic–plastic hypothesis should be considered under a purely academic profile for masonry material, since it is usually scarcely credible except for few particular cases. Nevertheless, it makes sense for comparison purposes with the EB and NT solutions.

Let denote by σ_{EB} and $\mathcal{C}_{\mathrm{EB}}$ the stress and the complementary energy values attained in the elastic–brittle solution, and by σ_{PL} and $\mathcal{C}_{\mathrm{PL}}$ the same quantities relevant to the elastic–plastic holonomic solution. Since $\sigma_{\mathrm{EB}} \leq \sigma_o'$, with σ_o' the tensile yield stress, and the elastic–plastic stress solution attains the minimum value of the energy functional between all the possible stress fields equilibrating the loads and with stresses lower than σ_o', one infers that

$$\mathcal{C}_{\mathrm{EB}} \geq \mathcal{C}_{\mathrm{PL}}. \tag{27}$$

Consequently, the elastic–plastic solution is closer than the EB solution to the elastic one, as regards the complementary energy. Figure 3c reports the contour lines of the objective function together with the elastic–plastic stress solution.

4 Boundary theorems on the EB stress solution

4.1 Upper bound and lower bound theorems for the EB stress solution

By coupling the inequalities inferred in Sect. 3 with reference to the four considered mechanical models (no-tension NT, elastic–brittle low-tension EB, elastic–plastic PL, and purely elastic EL), some bounding theorems may be formulated on the EB stress solution, concerning the relationships shown in the previous sections with the relevant stress solutions. The considered solutions have been shown to satisfy an order property with reference to the relevant energetic functionals of the type

$$\mathcal{C}_{\mathrm{NT}} \geq \mathcal{C}_{\mathrm{EB}} \geq \mathcal{C}_{\mathrm{PL}} \geq \mathcal{C}_{\mathrm{EL}}. \tag{28}$$

The following bounding theorems can thus be formulated concerning the EB stress solution:

(I) **Upper Bound Theorem**:

"In an elastic–brittle structure with tensile strength under mono-axial stress, the complementary energy functional attains a value that is upper-bounded in the solution by the complementary energy value relevant to the no-tension solution. The bound gets sharper as the limit tensile strength gets smaller".

(II) **Lower Bound Theorem**:

"In an elastic–brittle structure with tensile strength under mono-axial stress, the complementary energy functional attains a value that is lower-bounded in the solution by the complementary energy value relevant to the holonomic plastic (and a fortiori to the elastic) solution. The bound gets sharper as the limit tensile strength gets smaller".

It can be concluded that if the material is endowed with a low tensile strength σ_o', the difference between the NT and EB solutions can be neglected as σ_o' approaches zero.

4.2 Representation of the solutions and formulation outcomes

In Fig. 4, the complementary energy functional is represented through its contour lines where the functional is constant with decreasing values as one moves towards the central minimum point, together with the constraints imposed by the admissibility conditions relevant to the different materials.

One can observe that the elastic–plastic admissibility allows to identify the elastic–plastic domain $\mathbf{D}_{\mathrm{PL}}$ where the relevant solution σ_{PL} should be searched for, whilst the NT solution σ_{NT} should be searched for in the relevant statically admissible stress domain $\mathbf{D}_{\mathrm{NT}}$ that is, of course, included in $\mathbf{D}_{\mathrm{PL}}$.

In synthesis:

(i) the elastic solution σ_{EL} is attained at the unconstrained minimum point of the CE functional (Fig. 3a);
(ii) the no-tension solution σ_{NT}, since it should attain the minimum admissible value, is placed at the tangent point of the CE line tangent to the contour of the NT domain $\mathbf{D}_{\mathrm{NT}}$ (Fig. 3b);
(iii) the plastic solution σ_{PL}, since it should attain the minimum admissible value, is placed at the tangent point of the CE line tangent to the contour of the plastic domain $\mathbf{D}_{\mathrm{PL}}$ (Fig. 3c);
(iv) the elastic–brittle solution σ_{EB} is placed in the area bounded by the contour of the elastic–plastic domain $\mathbf{D}_{\mathrm{PL}}$ and the CE line relevant to the NT solution (Fig. 4).

Based on the above considerations, one may infer that:

- The EB solution belongs to the area bounded between the PL and the NT solutions, as shown in Fig. 4. If σ_o' is small (low-tension material), this area is very narrow, so that the difference between the NT and the EB solution fades away.
- That narrow area, which is a part of the region included between the two definition domains of the plastic and the NT solutions, gets even smaller as the tensile limit σ_o' of the material gets smaller, or it decreases because of the decay in time.
- When the yield tensile resistance is attained in the structure, the stress level is substantially very close to the NT case.
- Definitely for low-tension material, like in most masonry textures, the stress regimes relevant to the EB and the NT solutions are approximately the same, with the NT case working on the safe side from the point of view of structural assessment.

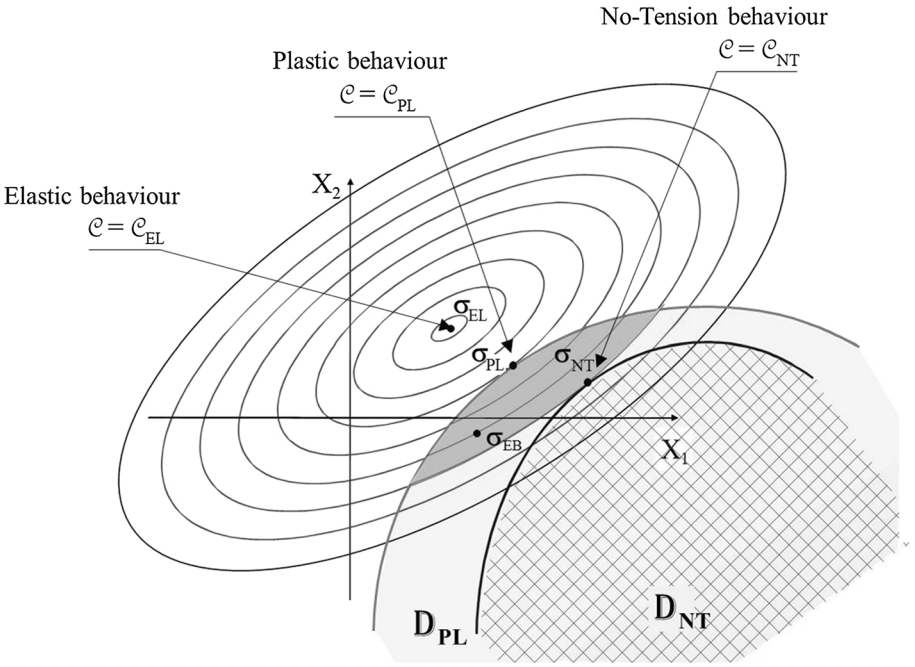

Fig. 4 CE optimum properties of the stress solutions

5 Conclusions

The paper introduces the formulation of an original mechanical model for masonry material, which is able to embed some skill of resisting tensile stresses; one also discusses its opportunity for safety assessment of masonry structures. Under this perspective, the presented elastic–brittle (EB) low-tension model aims at producing some improvement with respect to standard no-tension (NT) models, where no-tension is admitted by the material, still allowing the same fracture modes as the NT ones and an evolutionary behaviour tending to the NT one.

Since, by the reasons discussed in Sect. 1, as far as the sophistication of the model is increased, the computational effort required by the implementation of the model itself tends to become both cumbersome and unreliable for engineering purposes, it is of primary importance to recognise that the attempt to fit the material properties in details does not produce significant improvements.

The properties of the EB solution are investigated through the development of an original theoretical formulation starting from Eq. (14), which leads to the set-up of two bounding theorems, formulated in Sect. 4.1 for the EB stress solution.

In conclusion, after proving that the EB solution, in energetic terms, is upper-bounded by the NT solution and lower-bounded by the PL (elastic–plastic) solution, one may observe that the EB and NT solutions in practical cases turn to be very close to each other. They are indeed characterised by some approximately equal stress regimes, pushing towards the adoption of the less sophisticated model which, despite making the computational effort lighter, is able to offer a more stable solution with an improved engineering reliability of the consequent assessments.

References

1. Heyman, J.: The stone skeleton. J. Solids Struct. **2**, 249–279 (1966)
2. Bazant, Z.P., Li, Y.N.: Stability of cohesive crack model: part I: energy principles. J. Appl. Mech. **62**(12), 959–964 (1995)
3. Kooharian, A.: Limit analysis of voussoir (segmental) and concrete arches. J. Am. Concr. Inst. **24**, 317–328 (1952)
4. Heyman, J., Pippard, A.J.S.: The estimation of the strength of masonry arches. Proc. Inst. Civ. Eng. **69**(4), 921–937 (1980). doi:10.1680/iicep.1980.2177
5. Khludnev A.M., Kovtunenko V.A.: Analysis of cracks in solids. Advances in Fracture Mechanics, pp. 386. Computational Mechanics (2000). ISBN 978-1853126253

6. Andreu, A., Gil, L., Roca, P.: Computational analysis of masonry structures with a funicular model. J. Eng. Mech. **133**(4), 473–480 (2007)
7. Anthoine, A.: Homogenization of periodic masonry, plane stress, generalized plane strain or 3D modeling. J. Commun. Numer. Methods Eng. **13**(5), 319–326 (1997)
8. Baratta, A., Corbi, I., Corbi, O.: Stress analysis of masonry structures: arches, walls, and vaults. In: D'Ayala, Fodde E. (eds.) Structural Analysis of Historic Constructions: Preserving Safety and Significance, pp. 321–329. CRC Press (2008). ISBN 978-0-415-46872-5
9. Baratta, A., Corbi, I., Corbi, O.: Analytical formulation of generalized incremental theorems for 2D no-tension solids. J. Acta Mech. **226**(9), 2849–2859 (2015). doi:10.1007/s00707-015-1350-2
10. Baratta, A., Corbi, I., Corbi, O.: Stability of evolutionary brittle-tension 2D solids with heterogeneous resistance. J. Comput. Struct. (2015). doi:10.1016/j.compstruc.2015.10.004
11. Baratta, A., Corbi, I., Corbi, O., Rinaldis, D.: Experimental survey on seismic response of masonry models. In: Proceedings of the 6th International Conference on Structural Analysis of Historic Constructions: Preserving Safety and Significance, SAHC08, Bath, 2–4 July 2008, 8, pp. 799–807, (2008). ISBN 0415468728;978-041546872-5
12. Baratta, A., Corbi, I.: Equilibrium models for helicoidal laterally supported staircases. J. Comput. Struct. (2013). doi:10.1016/j.compstruc.2012.11.007. ISSN 00457949
13. Baratta, A., Corbi, O.: Heterogeneously resistant elastic–brittle solids under multi-axial stress: fundamental postulates and bounding theorems. J. Acta Mech. **226**(6), 2077–2087 (2015). doi:10.1007/s00707-015-1299-1
14. Baratta, A., Corbi, O.: Contribution of the fill to the static behaviour of arched masonry structures: theoretical formulation. J. Acta Mech. **225**(1), 53–66 (2014). doi:10.1007/s00707-013-0935-x
15. Drosopoulos, G.A., Stavroulakis, G.E., Massalas, C.V.: Limit analysis of a single span masonry bridge with unilateral frictional contact interfaces. J. Eng. Struct. **28**(13), 1864–1873 (2006)
16. Fanning, P.J., Boothby, T.E.: Three-dimensional modelling and full-scale testing of stone arch bridges. J. Comput. Struct. **79**(29–30), 2645–2662 (2001)
17. Foti, D., Diaferio, M., Giannoccaro, N.I., Mongelli, M.: Ambient vibration testing. dynamic identification and model updating of a historic tower. NDT E Int. **47**, 88–95 (2012).doi:10.1016/j.ndteint.2011.11.009. ISSN:0963-8695
18. Furtmüller, T., Adam, C.: Numerical modeling of the in-plane behaviour of historical brick masonry walls. J. Acta Mech. **221**(1–2), 65–77 (2011). doi:10.1007/s00707-011-0493-z
19. Füssl, J., Lackner, R., Eberhardsteiner, J., Mang, H.A.: Failure modes and effective strength of two-phase materials determined by means of numerical limit analysis. J. Acta Mech. **195**(1–4), 185–202 (2008). doi:10.1007/s00707-007-0550-9
20. Pietruszczak, S., Ushaksaraei, R.: Description of inelastic behaviour of structural masonry. Int. J. Solids Struct. **40**(15), 4003–4019 (2003). doi:10.1016/S0020-7683(03)00174-4
21. Vintzileou, E.: Testing historic masonry elements and/or building models. J. Geotech. Geol. Earthq. Eng. **34**, 267–307 (2014)
22. Baratta, A., Corbi, O.: Closed-form solutions for FRP strengthening of masonry vaults. J. Comput. Struct. **147**, 244–249 (2015). doi:10.1016/j.compstruc.2014.09.007
23. Baratta, A., Corbi, I., Corbi, O.: Bounds on the Elastic Brittle solution in bodies reinforced with FRP/FRCM composite provisions. J. Compos. Part B Eng. **68**, 230–236 (2015). doi:10.1016/j.compositesb.2014.07.027
24. Elmalich, D., Rabinovitch, O.: Nonlinear analysis of masonry arches strengthened with composite materials. J. Eng. Mech. **136**(8), 996–1005 (2010). doi:10.1061/(ASCE)EM.1943-7889.0000140
25. Baratta, A., Corbi, I., Corbi, O.: Algorithm design of an hybrid system embedding influence of soil for dynamic vibration control. J. Soil Dyn. Earthq. Eng. **74**, 79–88 (2015)
26. Corbi, I., Corbi, O.: Macro-mechanical modelling of pseudo-elasticity in shape memory alloys for structural applications. J. Acta Mech. (2016). doi:10.1007/s00707-016-1624-3